Spectrochimica Acta Part A 75 (2010) 693–701

Contents lists available at ScienceDirect

Spectrochimica Acta Part A: Molecular and Biomolecular Spectroscopy

journal homepage: www.elsevier.com/locate/saa

Spectroscopic study of 2-, 4- and 5-substituents on pK_a values of imidazole heterocycles prone to intramolecular proton-electrons transfer

Abiodun O. Eseola [a,b,*], Nelson O. Obi-Egbedi [c]

[a] Chemical Sciences Department, Redeemer's University, Redemption City, Km. 46 Lagos – Ibadan Expressway, Nigeria
[b] Beijing National Laboratory for Molecular Science, Institute of Chemistry, Chinese Academy of Sciences, Beijing, 100190, China
[c] Chemistry Department, University of Ibadan, Ibadan, Nigeria

ARTICLE INFO

Article history:
Received 19 September 2009
Received in revised form
12 November 2009
Accepted 17 November 2009

Keywords:
Ionization constants
UV spectroscopy
pK_as
Protonation–deprotonation
Substituent effects

ABSTRACT

New 2-(1H-imidazol-2-yl)phenols (**L1Et**–**L8*t*BuPt**) bearing a phenolic proton in the vicinity of the imidazole base were prepared and characterized. Experimental studies of the dependence of their protonation/deprotonation equilibrium on substituent identities and intramolecular hydrogen bonding tendencies were carried out using electronic absorption spectroscopy at varying pH values. In order to make comparison, 2-(anthracen-10-yl)-4,5-diphenyl-1H-imidazole (**L9Anthr**) bearing no phenolic proton and 4,5-diphenyl-2-(4,5-diphenyl-1H-imidazol-2-yl)-1H-imidazole (**L10BisIm**) bearing two symmetrical imidazole base fragments were also prepared and experimentally investigated. DFT calculations were carried out to study frontier orbitals of the investigated molecules. While electron-releasing substituents produced increase in protonation–deprotonation pK_as for the hydroxyl group, values for the imidazole base were mainly affected by polarization of the imidazole ring aromaticity across the 2-imidazole carbon and the 4,5-imidazole carbons axis of the imidazole ring. It was concluded that electron-releasing substituents on the phenol ring and/or electron-withdrawing substituents on 4,5-imidazole carbons negatively affects donor strengths/coordination chemistries of 2-(1H-imidazol-2-yl)phenols, and vice versa. Change of substituents on the phenol ring significantly altered the donor strength of the imidazole base. The understanding of pK_a variation on account of electronic effects of substituents in this work should aid the understanding of biochemical properties and substituent environments of imidazole-containing biomacromolecules.

1. Introduction

For the past many decades, interest in the understanding of factors controlling the mechanisms of reactions of biological and medicinal interests has been sustained [1–5]. Coupled proton-electron transfer is a subject of significant current interest [6–9] and physicochemical data such as ionization constant values (often derived as pK_as) are routinely employed in characterizing biomolecules such as metalloenzymes, amino acids, etc. The pK_a of a drug is one of the most important parameters employed to explain its physicochemical behaviour and acid-base properties, and to study pharmaceutical pre-formulations [10]. Changes in pK_a values in biological macromolecules are often investigated to establish modes of interactions between an acid or base fragment and its neighbouring functional groups [11]. However, in the presence of supramolecular folding that exists in biological macromolecules, investigation of behaviours of pH sensitive functions is hindered. Small, well-characterized, organic molecules provide access to understanding of phenomena observed in the macrostructures. Spectroscopic determination of ionization constant of weak acids or bases is of widespread application and considered suitable even at extremes of pH, poor solute solubilities and for species prone to conformational photo-tautomerism [11–13]. Aqueous–organic mixtures are often employed for various pH buffers in ionization constant determinations [10].

Moieties such as adenine, guanine, histidine, etc., contain imidazole functions and are involved in intramolecular and intermolecular chemistries of biological macromolecules under pH specific conditions [14–18]. Imidazole base of histidine is recognized to be an interesting ligand in the bioinorganic chemistry of most heamoptoteins of which investigation of basicity and steric effects gives understanding of the role of the leaving group in controlling mechanisms [9,19]. In previous studies on histidine, it is believed that pK_a values assigned to the imidazole ring (p$K_a \approx 6$) is distinguishable from values ascribed to carboxy (p$K_a \approx 2$) or amino (p$K_a \approx 9$) functionalities [1,2,11]. However, pK_a values of some

* Corresponding author at: P.M.B. 3005, Redemption City, Ogun State – Nigeria. Tel.: +234 7062192104.
E-mail addresses: bioduneseola@run.edu.ng, bioduneseola@hotmail.com (A.O. Eseola).

1386-1425/$ – see front matter © 2009 Elsevier B.V. All rights reserved.
doi:10.1016/j.saa.2009.11.041

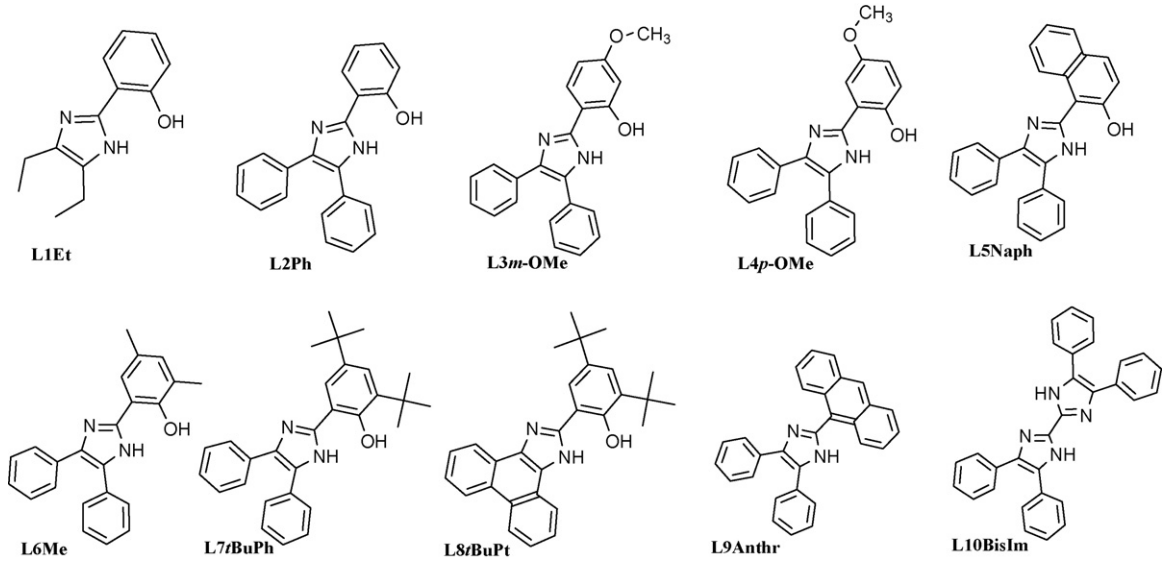

Scheme 1. Molecular frameworks investigated in this work.

imidazole bases have been reported to be inaccessible within the pH scale range [20]. On account of protonation–deprotonation reactions, spectroscopic behaviour of imidazole base chromophores have attracted considerable attention towards potential pH sensory and fluorescence switching applications [21–29]. Proper understanding of donor–acceptor properties of imidazole bases in the presence of different neighbouring functionalities is still lacking. As discussed in our previous report on ^{1}H NMR comparison [30], protonation and deprotonation schemes have been concluded for an oxazole system which the authors wrongly thought to be an imidazole ligand [29]. Progress has been made in the understanding Excited State Intramolecular Proton-electron Transfer (ESIPT) phenomenon of 2-(imidazol-2-yl)phenols [31–35]. However, such studies have been largely restricted to 2-(1H-benzo[*d*]imidazol-2-yl)phenols with scarce knowledge of substituent and solute media effects. In preceding experiments recently published on a series of ligands and their corresponding zinc complexes involving some of the compound in the present studies, the role of substituents and solvents media in preventing ESIPT was presented and changing solvent polarities from tetrahydrofuran (THF, dielectric constant ≈7) to dimethylformamide (DMF, dielectric constant ≈38) yielded little or no change on absorption peak positions (i.e. 0–2 nm shifts). However, observed shifts in photoluminescence maxima (spread over 1–57 nm) for the reported imidazole-phenol ligands as a result solvent variation (from THF to DMF) indicated that significant change in polarities for polar solvents produced significant modification of excited state electronic characteristics while having insignificant effects on the ground state electronic structures [36]. Calculational reports also largely restricted to 2-(1H-benzo[*d*]imidazol-2-yl)phenols are known [37,38]. The B3LYP/6–311 + G* basis set has been successfully employed as a reliable method in DFT calculations of imidazole organic systems [39]. Investigation of the consequence of intramolecular proton–base interactions on physicochemical parameter such as ionization constants of the proton donor as well as the acceptor is unknown.

Owing to importance of imidazole bases, attention has been drawn to investigation of small molecules containing imidazole nucleus, and such studies are yet few. Moreover, works involving a series of imidazole bases with differing substituent environment is also scarce. Particularly, studies of substituent environments on ionization constants of imidazoles prone to intramolecular proton–electron transfer have not been reported. Herein, we present our results on syntheses and spectroscopic investigation of ionization constants for a series of 2-aryl-1H-imidazoles. Two imidazole molecules that lack intramolecular proton–electron transfer capacities have been included for comparison. Calculated properties based on optimized geometries of the molecules as well as experimental ^{1}H NMR and FTIR data of active protons were discussed in attempt to rationalize observed variations in ionization constants (Scheme 1).

2. Experimental

2.1. General considerations

All manipulations of oxidation-prone reactions were performed under nitrogen atmosphere using standard Schlenk techniques. All starting materials were obtained commercially as reagent grades and used without further purification. **L1Et**, **L2Ph**, **L3*m*-**

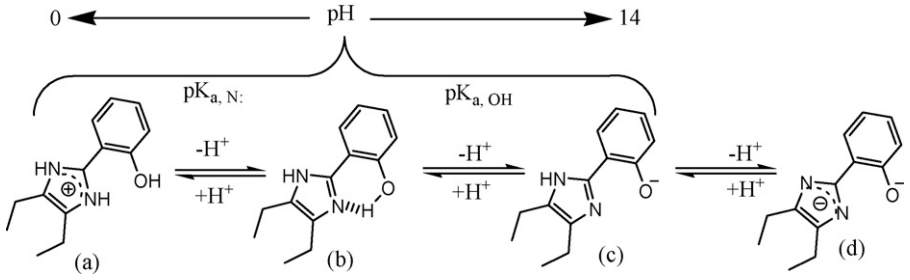

Scheme 2. Possible protonation states for base and active proton components. (a), (b) and (c) were observed within pH 0–14.

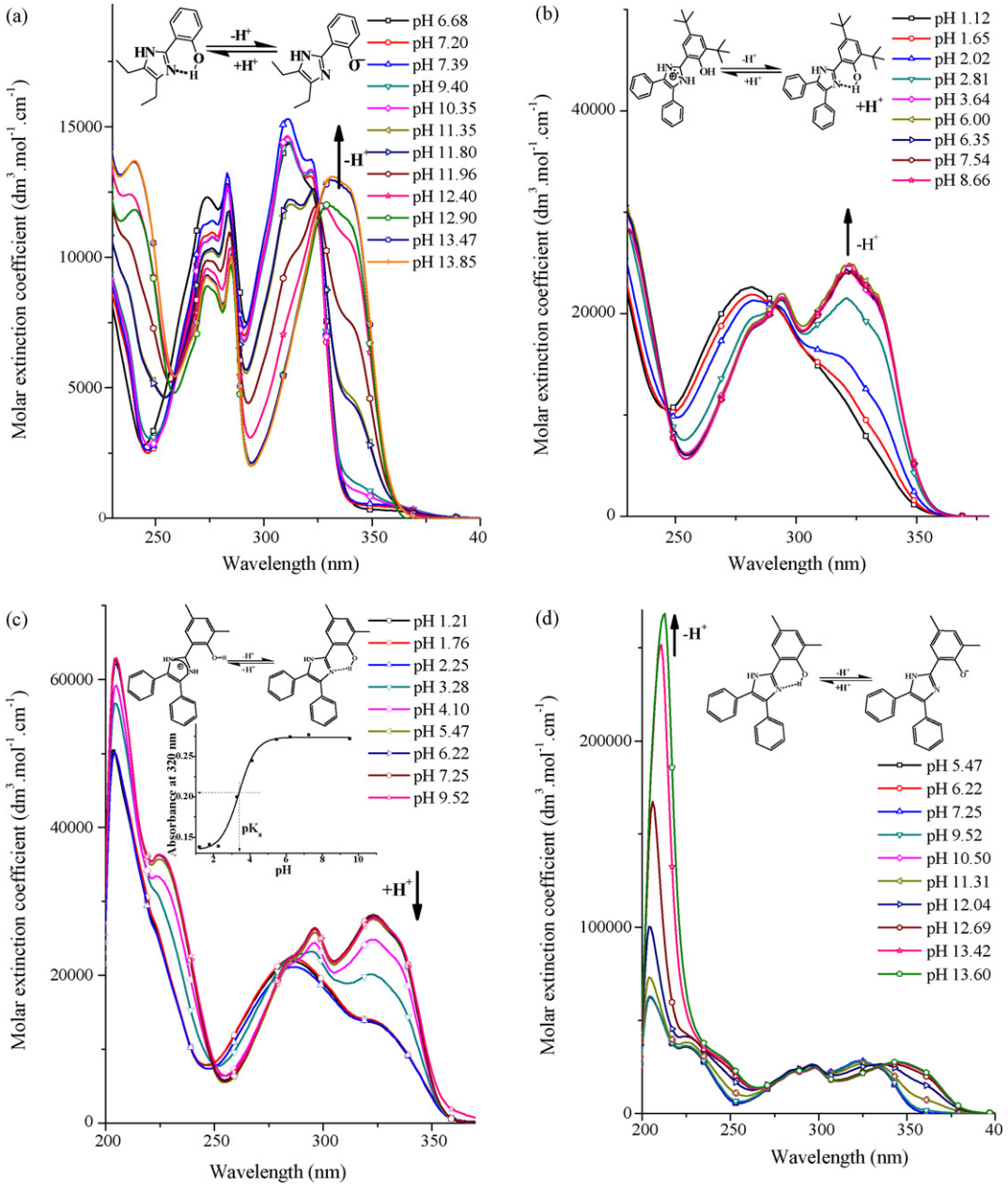

Fig. 1. Overlays of absorption spectra at different pH values for (a) **L1Et**, (b) **L7*t*BuPh** and (c and d) **L6Me**.

OMe, **L4*p*-OMe**, **L6Me**, **L7*t*BuPh** and **L8*t*BuPt** were prepared according to recently published procedures [36]. The synthesized organic compounds were purified on silica gel column to exclude impurities. Elemental analyses were performed on a Flash EA 1112 microanalyzer. ^{1}H and ^{13}C NMR spectra were recorded on a Bruker ARX-400 MHz instrument using deuterated chloroform as solvent and TMS as internal standard. IR spectra were recorded on a Nicolet 6700 FT-IR spectrometer as KBr discs in the range of 4000–600 cm^{-1}. UV–vis measurements were recorded on Shimadzu 1600 Spectrophotometer. The pK_a determination experiments were done using ≈10^{-5} M solutions of the compounds in ethanol–water mixture which consists of 70% absolute ethanol and 30% distilled water. Calculated amount of potassium chloride was used to achieve 0.1 M concentration of the salt in order to maintain fairly constant ionic strength and the pH of solutions were adjusted with the aid of a calibrated pH meter and through addition of potassium hydroxide or hydrochloric acid solutions. Optimized geometries and calculated properties were obtained through DFT calculations conducted at the B3LYP/6–311 + G* level with input files created based on simulated dielectric constants for 70% ethanol–water mixture. DFT calculations were obtained using Gaussian 98 package of programs [41].

2.2. Preparation of imidazoles

1-(4,5-Diphenyl-1H-imidazol-2-yl)naphthalen-2-ol **(L5Naph)**: Benzil (2.00 g, 9.51 mmol), 2-hydroxynaphthalene-1-carbaldehyde (1.64 g, 9.51 mmol) and ammonium acetate (14.67 g) refluxed for 2 h in 10 mL glacial acetic acid. The reaction mixture was allowed to cool, transferred to 40 mL water, carefully neutralized with concentrated aqueous ammonia and the crude product filtered. After washing with water, the dried solid was recrystallized from ethanol to yield the **L5Naph** as yellow micro-needles (2.23 g, 64.7%). Selected IR peaks (KBr disc, cm^{-1}): ν 3245vs, 3052m,

Table 1
Experimental FTIR, ^{1}H NMR, UV absorption and pK_a data of studied imidazole molecules.

Compds	FTIR and NMR signals				λ_{max} (nm) [ε (dm^3/mol cm)][a]			Ionization constant	
	ν_{N-H} (cm^{-1})[b]	ν_{O-H} (cm^{-1})[b]	^{1}H δ_{N-H} (ppm)[c]	^{1}H δ_{O-H} (ppm)[c]	Cation	Neutral	Anion	p$K_{a,N} \pm S$	p$K_{a,OH} \pm S$[d]
L1Et	3256vs (sh)	3360m (br)[e]	NO[f]	NO[f]	313 [12,900]	311 [15,350]	332 [12,770]	6.64 ± 0.07	11.91 ± 0.10
L2Ph	3208vs (sh)	NO[f]	12.83 (br)	9.37 (br)	315 [28,730]	317 [43,140]	338 [38,750]	4.22 ± 0.10	10.05 ± 0.08
L3*m*-OMe	3217vs (sh)	NO[f]	12.90 (vbr)	9.14 (vbr)	317 [44,150]	317 [49,870]	335 [46,560]	4.47 ± 0.16	10.25 ± 0.05
L4*p*-OMe	3205vs (sh)	NO[f]	NO[f]	NO[f]	341 [11,070]	334 [18,040]	356 [16,040]	3.64 ± 0.09	10.81 ± 0.14
L5Naph	3243vs (sh)	NO[f]	NO[f]	NO[f]	336 [6700]	344 [9450]	379 [10,960]	5.38 ± 0.01	10.50 ± 0.02
L6Me	3256vs (sh)	3320s (br)[e]	NO[f]	9.26 (br)	320 [13,790]	323 [28,360]	345 [27,680]	3.38 ± 0.07	11.64 ± 0.09
L7*t*BuPh	**3427vs (sh)**	**3450m (br)[e]**	**13.06 (vbr)**	**9.24 (vbr)**	281 [22,400]	322 [24,220]	335 [21,580]	**2.28 ± 0.04**	**13.47 ± 0.02**
L8*t*BuPt	**3478s (sh)**	**3510w (br)[e]**	**13.48 (sh)**	**9.92 (sh)**	298 [17,850]	335 [24,010]	336 [23,730]	**1.11 ± 0.02**	**13.04 ± 0.08**
L9Anthr	3383m (sh)	NA[g]	9.29	NA[g]	370 [10,330]	365 [10,200]	–	5.46 ± 0.04	NA[g]
L10BisIm	3440s (br)	NA[g]	NO[f]	NA[g]	–	336 [12,700]	–	NO[f]	NA[g]

[a] λ_{max} = the longest wavelength absorption band maximum at the various protonation states.
[b] Solid state in KBr disc.
[c] In deuterated chloroform.
[d] *S* represents standard error.
[e] Extends under the O–H peak. sh = sharp, br = broad, s = strong, vs = very strong, ν = vibrational frequency in cm^{-1}, ^{1}H δ = proton chemical shift in ppm.
[f] NO = not observed.
[g] NA = not applicable.

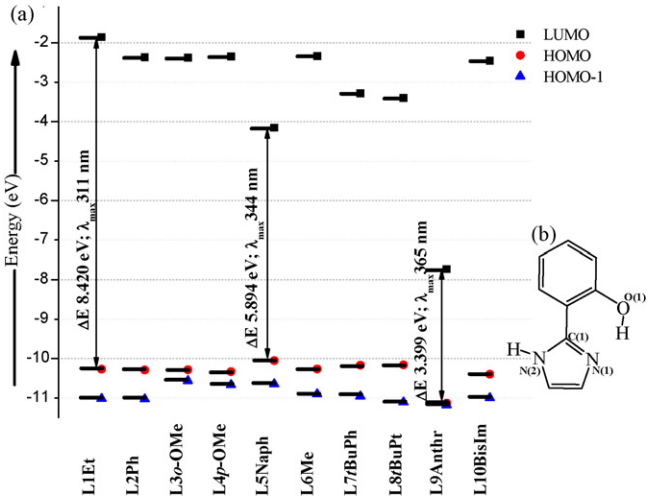

Fig. 2. (a) Energy separation between LUMO, HOMO and HOMO-1 energy levels in the studies molecules and (b) atoms labeling scheme for Mulliken charges reported in Table 2.

1667w, 1619s, 1598s. ^{1}H NMR (400 MHz, TMS, $CDCl_3$); δ 8.21 (d, J = 8.4 Hz, 1H); 7.86 (d, 8.0 Hz, 1H), 7.79 (d, 8.8 Hz, 1H); 7.62 (d, 7.2 Hz, 4H); 7.57 (dd, 7.2 Hz, 1H); 7.39 (m, 7H). ^{13}C NMR (400 MHz, $CDCl_3$, TMS); 157.52, 145.73, 130.57, 128.74, 127.79, 123.06, 118.95, 117.85, 112.47. Anal. calc. for $C_{25}H_{18}N_2O.0.2H_2O$ (M. wt., 444.12): C, 82.21; H, 5.17; N, 7.57. Found: C, 82.43; H, 5.64; N, 7.13.

2-(Anthracen-9-yl)-4,5-diphenyl-1H-imidazole (**L9Anthr**): Benzil (0.21 g, 0.98 mmol), 9-anthraldehyde (0.20 g, 0.98 mmol) and ammonium acetate (1.51 g, 19.60 mmol) were refluxed in glacial acetic acid (3 mL) for 2 h. The cooled reaction solution was diluted with cc. 10 mL water, carefully neutralized using concentrated aqueous ammonia and the precipitate filtered, washed with distilled water and the crude precipitate was extracted into dichloromethane. The organic extract was purified on silica gel column using petroleum ether:dichloromethane:ethyl acetate in 10:3:1 ratio to obtain **L9Anthr** as yellow micro-needles (0.37 g, 95%). Selected IR peaks (KBr disc, cm^{-1}): ν 3383s, 3053vs, 1606s, 1529s, 1505s. ^{1}H NMR (400 MHz, TMS, $CDCl_3$); δ 9.29 (s, 1H, imidazole); 8.54 (s, 1H, anthr.), 8.02 (d, J = 9.6 Hz, 4H, anthr.); 7.80 (br, 2H, anthr.); 754 (br, 2H, anthr.); 7.46 (m, 4H, phenyl); 7.34 (br, 6H, phenyl). Anal. calc. for $C_{25}H_{18}N_2O.0.2H_2O$ (M. wt., 444.12): C, 82.21; H, 5.17; N, 7.57. Found: C, 82.43; H, 5.64; N, 7.13.

4,5-Diphenyl-2-(4,5-diphenyl-1H-imidazol-2-yl)-1H-imidazole (**L10BisIm**): Benzil (5.00 g, 23.80 mmol), ammonium acetate (25.00 g, 356.74 mmol) and glacial acetic acid (20 mL) were heated under reflux condition and, while under reflux, glyoxal water (2.7 mL, 23.78 mmol) was added over 20 min. Reflux was allowed to continue for 2 h 30 min. followed by cooling, dilution in ≈50 mL water and neutralization with concentrated aqueous ammonia solution. The aqueous solution was decanted from the brown, gummy residue was extracted using dichloromethane and purified on silica gel column using petroleum ether/ethyl acetate in ration 10:1. Pure product was obtained as white micro-crystals (<5% yield). Selected IR peaks (KBr disc, cm^{-1}): ν 3440s, 3050m, 1620w, 1578w, 1389vs, 765vs. ^{1}H NMR (400 MHz, TMS, $CDCl_3$); δ 7.46 (m, 8H); 7.33 (m, 12H). Anal. calc. for $C_{30}H_{22}N_4{\cdot}(1/2)H_2O$: C, 80.51; H, 5.18; N, 12.52. Found: C, 80.55; H, 5.37; N, 12.35.

3. Results and discussion

3.1. Absorption properties at different protonation states

Table 1 contains the experimental spectral and pK_a data for the investigated molecules. For reliable determination of pK_a values,

Table 2
Ligand dipole moments, LUMO–HOMO separations and Mulliken charge densities of selected atoms determined at the B3LYP/6–311 + G* level.

Ligands	DM (D)[a]	$\Delta E_{(LUMO)-(HOMO)}$ (eV)[b]	Mulliken charge densities (Q)				
			N(1)	N(2)	N(1)–N(2)	O(1)	C(1)
L1Et	5.865	8.420	−0.616	−0.478	0.138	−0.223	0.458
L2Ph	5.869	7.927	−0.613	−0.491	0.122	−0.214	**0.462**
L3*m*-OMe	3.292	7.907	−0.621	−0.498	0.123	**−0.209**	**0.471**
L4*p*-OMe	4.784	7.993	−0.603	−0.488	0.115	**−0.222**	**0.452**
L5Naph	5.283	**5.894**	−0.642	−0.489	0.164	−0.204	0.488
L6Me	5.511	7.928	**−0.616**	**−0.492**	0.124	**−0.223**	**0.442**
L7*t*BuPh	6.020	6.881	**−0.623**	**−0.491**	0.132	**−0.245**	**0.439**
L8*t*BuPt	5.183	6.784	**−0.630**	**−0.537**	0.089	**−0.234**	**0.434**
L9Anthr	**2.627**	**3.399**	−0.542	−0.495	**0.048**	NA[c]	0.473
L10BisIm	**0.347**	7.951	−0.459	−0.412	**0.047**	NA[c]	0.451

[a] Dipole moments in Debye.
[b] LUMO = lowest unoccupied molecular orbital; HOMO = highest occupied molecular orbital. eV = electron Volts. Selected atomic labels correspond to notations according to Fig. 4(b).
[c] NA = not applicable.

it is desirable to have absorption bands that are significantly distinguishable at the different protonation states. Fortunately, the protonation–deprotonation reactions in this work afforded species with different absorption band positions and/or shapes (Scheme 2, Fig. 1). Three protonation states were observed within pH 1–14, which corresponds to imidazolium cation (lower pH end), neutral imidazole-phenol (pH ≈5–9) and imidazole-phenolate anion (higher pH end). Use of spectral absorption methods in quantifying concentrations of equilibrium species in solution has been known to render reliable results [40]. The ionization constants were obtained as pK_a on the basis of Henderson–Hasselbalch theory:

$$\mathrm{pH} = \mathrm{p}K_a - \log \frac{A - A_0}{A_f - A}$$

where A_0 and A_f represent the initial and final absorbance values for the various protonated–deprotonated species, respectively. Though solutions of similar concentrations were planned, wide variation in extinction coefficients were observed due to substituent variations. Similar trend was also observed in substituent effects on THF solution for some of the ligands studied [36]. The pK_a values were obtained from sigmoidal fittings on plots of absorbance values at wavelengths of maximum difference between the absorbance of protonated and deprotonated forms against pH (inset, Fig. 1(c)). R^2 values were in the range 0.9744–0.9997.

It is noteworthy that the longest wavelength absorption bands of the imidazole-phenol ligands progressively exhibited red shift on transforming from the imidazolium forms into the

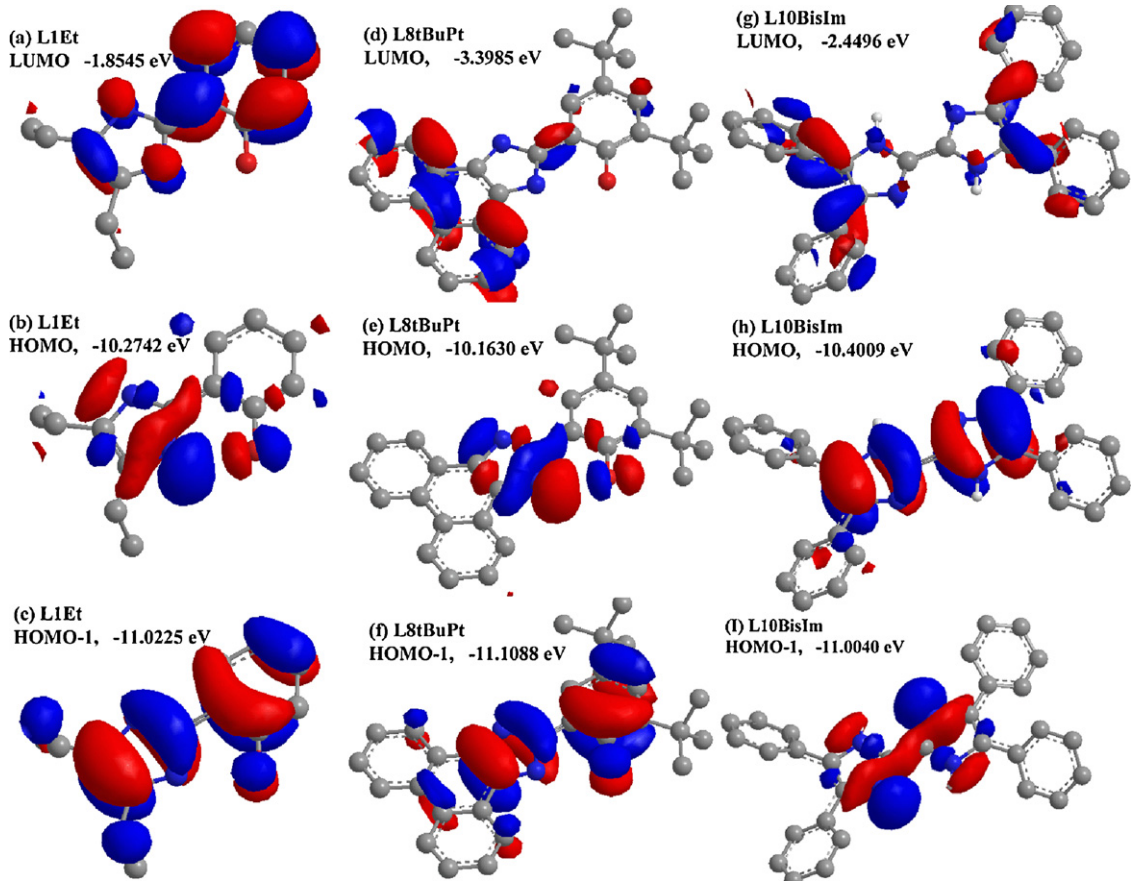

Fig. 3. Optimized structures of **L1Et** (a–c), **L8*t*BuPt** (d–f) and **L10BisIm** (g–i) showing the frontier molecular orbitals at LUMO, HOMO and HOMO-1 levels. Hydrogen atoms were omitted for clarity.

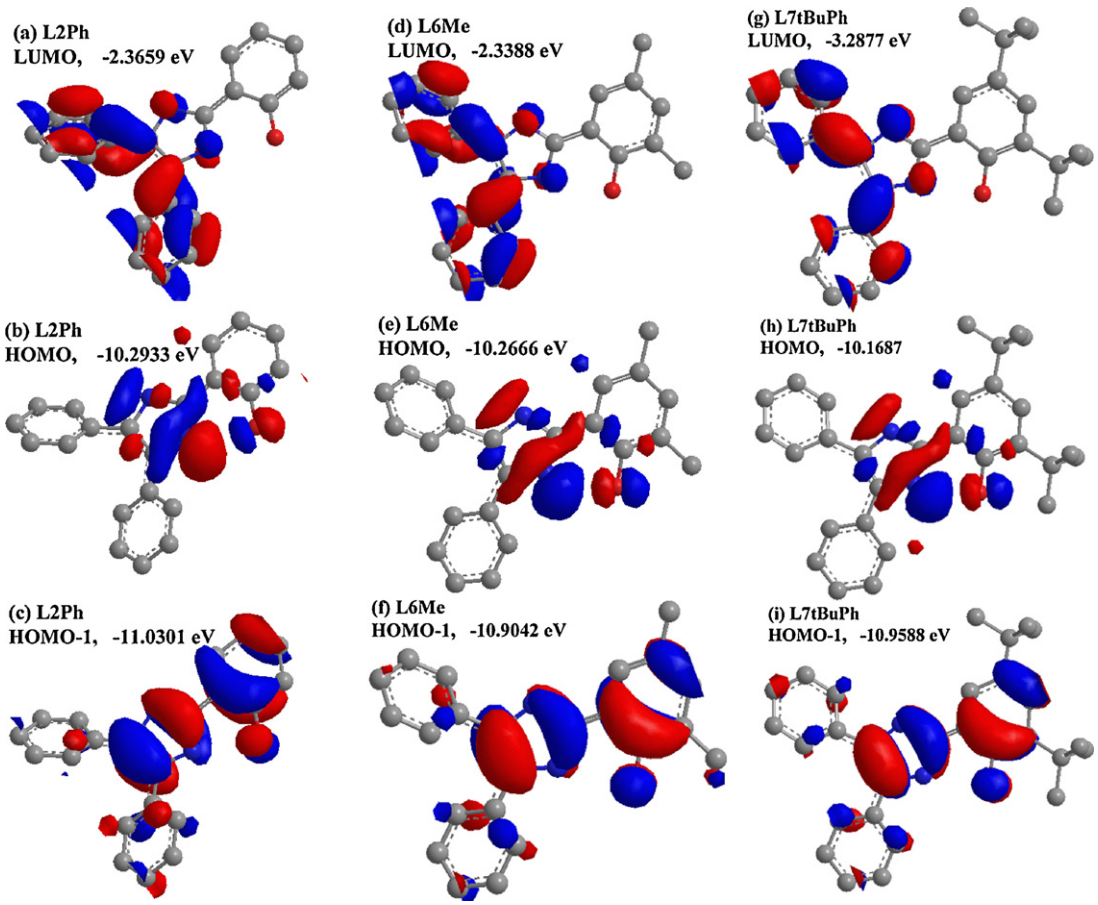

Fig. 4. Optimized structures of **L2Ph** (a–c), **L6Me** (d–f) and **L7*t*BuPh** (g–i) showing the frontier molecular orbitals at LUMO, HOMO and HOMO-1 levels. Hydrogen atoms were omitted for clarity.

neutral species and into the phenolate forms (Table 1). However, absorption maxima of the second absorption bands were less sensitive to the protonation–deprotonation events except for gradual changes in absorbance or peak position (Fig. 1(a)). Also notable is the observed sudden jump in molar extinction coefficient (≈×5) of the shortest wavelength band of the imidazole-phenols (≈220 nm) at higher alkalinities (pH ≈12–14), which was accompanied by relatively little or no change in intensity of the longer wavelength bands (Fig. 1(d)). This observation may be of value to pH sensory research. The bis-imidazole molecule **L10BisIm** showed no change in absorption characteristics over pH 1–14. This observation is attributable to the symmetrical nature of the ligand and consequent lack of dipole tendencies. This view is supported by the broad ν_{N-H} frequency due to fast intramolecular proton transfers between the two imidazole nitrogen atoms (Fig. 4(d)). The pK_a values for **L10BisIm** probably exist outside the pH scale range. DFT calculations on the series of molecules showed good inverse agreement between trends of S_0–S_1 absorption peak wavelengths (nm) and the energy separations between respective highest occupied molecular orbitals (HOMO) and lowest unoccupied molecular orbitals (LUMO) levels (e.g. **L1Et**: $\Delta E_{(LUMO)-(HOMO)} = 8.420$ eV, $\lambda_{max} = 311$ nm; **L5Naph**: $\Delta E_{(LUMO)-(HOMO)} = 5.894$ eV, $\lambda_{max} = 344$ nm; **L9Anthr**: $\Delta E_{(LUMO)-(HOMO)} = 3.399$ eV, $\lambda_{max} = 365$ nm; Fig. 2; Table 2).

3.2. Substituent effects and trends in pK_a values

Increase in electron-releasing capacity of the phenol ring towards the 2-position of the imidazole ring or increase in electron-withdrawing character of substituents on the 4,5-imidazole carbons simultaneously produced lowering of imidazole base pK_as and increase of the phenolic hydroxyl group pK_as (Table 1; **L1Et**: 6.64–11.91; **L6Me**: 3.38–11.64; **L7*t*BuPh**: 2.28–13.47; **L8*t*BuPt**: 1.11–13.04). The separation in pK_a values produced by a combination of push–pull substituents, which was achieved through *t*Bu and 4,5-diphenyl or phenanthreneyl substitution as in the cases of compounds **L7*t*BuPh** and **L8*t*BuPt**, is notable. In other words, as the π-electron cloud of the imidazole ring is shifted from the 2-carbon towards the 4,5-carbons, it's protonation–deprotonation equilibrium constant becomes larger (i.e. lower pK_a values). This implies that the donor ability of the imidazole base is reduced and effective protonation of species in solution could only be achieved in lower pH media (i.e. higher $[H^+]$). Calculated charge densities revealed a decrease in positive charge density on the 2-imidazole carbon which suggests a push of negative charge from the phenol ring towards the imidazole ring in the order **L2Ph** (0.462) > **L6Me** (0.442) > **L7*t*BuPh** (0.439) > **L8*t*BuPt** (0.432 having a combination of push and pull) (Table 2). Increase in the calculated electronic density on the oxo-atom of the phenol group also indicates expected push of electron density towards 2-imidazole position in the order **L7*t*BuPh** (−0.245) > **L6Me** (−0.223) > **L2Ph** (−0.214). Furthermore, the electron-releasing group on the phenol ring strengthened the phenolic O–H bond as established by FTIR data (Table 1) and a weaker strength of intramolecular H-bonding is thus implied. Increasing pK_a values for the deprotonation equilibrium of phenolic O–H on account of greater electron-releasing character of phenol ring substituents is in support of the consequent strengthening of O–H bonds. The pK_a data in the present work also provides understanding towards metal–organic chelation reactivity of 2-(1H-imidazol-2-yl)phenols. A combination of

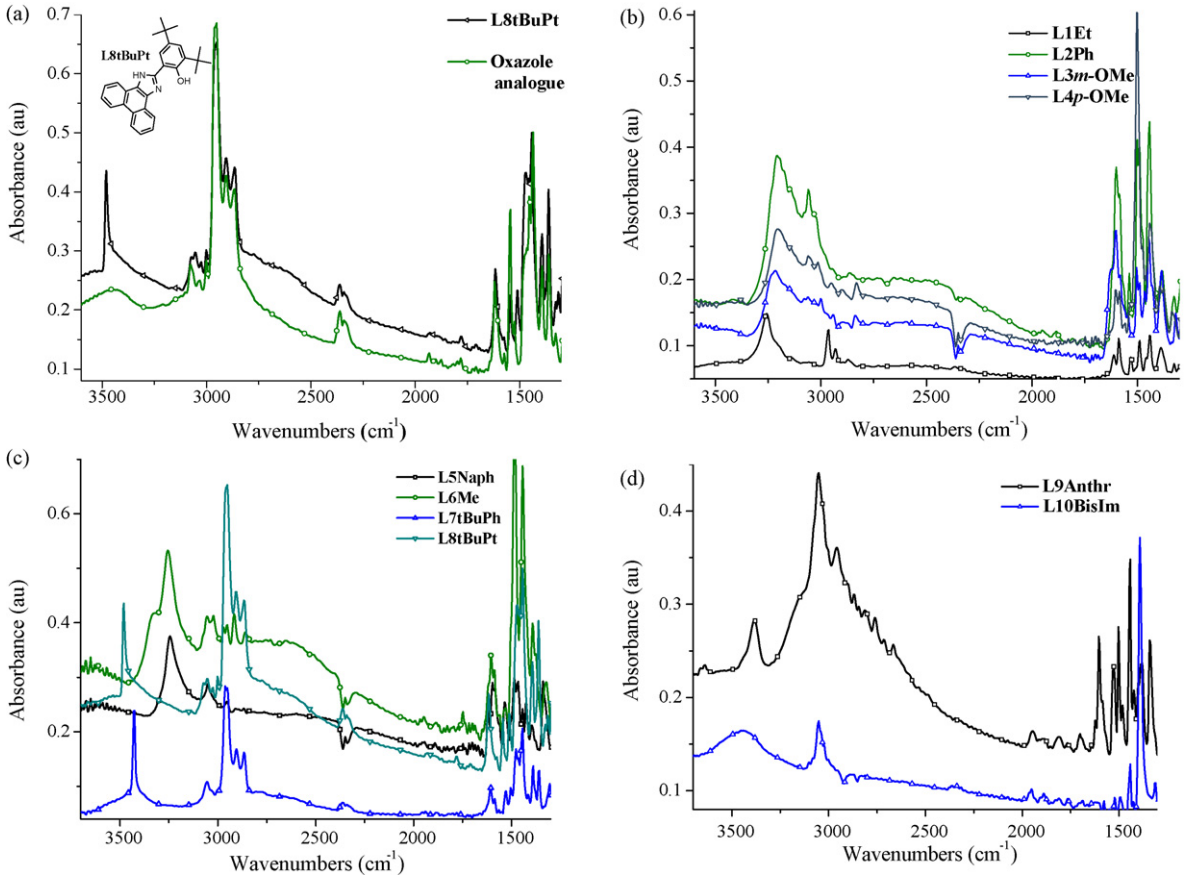

Fig. 5. (a–d) Solid-state FTIR spectra (as KBr disc) of studied molecules in this work.

push–pull substituents as in **L7*t*BuPh** and **L8*t*BuPt** leads to poor imidazole N-donor strength and tougher phenolic O–H deprotonation. As observed in previously published work [36], coordination of **L7*t*BuPh** and **L8*t*BuPt** with zinc(II) ion was achieved only in the presence of triethylamine base. The product yield was quite low and the complexes decomposed in polar-protic solvents.

Relative to the pK_a data for **L2Ph**, data for **L4*p*-OMe** suggest that the electron-rich methoxy group *para*- to the hydroxyl function is electron-releasing towards the imidazole ring in contrast to substituent effect of the methoxy group on **L3*m*-OMe**. Mulliken positive charges on the 2-carbon of the imidazole ring, which decreased for **L4*m*-OMe** (0.452) and increased for **L3*m*-OMe** (0.471) relative to **L2Ph** (0.462), agrees with the observed opposite effects of *o*- and *p*-methoxy substitution. Observed data for **L5Naph** suggest that extension of conjugation on the naphthol group yielded reduction in charge shift towards imidazole ring. Experimental data suggest that the fused phenanthrene group (**L8*t*BuPt**) on the 4,5-carbons of the imidazole behaved as electron-withdrawing. While 4,5-diphenyl groups acted to a lesser extent as electron-withdrawing, the 4,5-diethyl groups showed electron-releasing character. The electron-withdrawing roles of the phenanthreneyl and 4,5-diphenyl groups can be attributed to π-interactions between the aromatic π-electrons of the substituents and that of the imidazole ring. The optimized structure of the 4,5-diphenyl substituted compound (Fig. 4) revealed π-electron delocalization over the C–C single bonds between imidazole ring and the aromatic substituents at 4-, 5- and 2-positions. Moreover, optimized structure computation for **L1Et** showed a double bond character between the 2-imidazole carbon and phenol rings. In agreement with published X-ray structures of **L1Et** and **L6Me** [36], it was observed that the C–C bond lengths between the 4- or 5-carbon of the imidazole ring and the substituent ethyl groups are typical of single bonds (average of 1.507 Å), while the corresponding lengths to the phenyl substituted analogue indicated some extent of resonance conjugation across the C–C bond (average of 1.475 Å). Fig. 3 presents frontier orbital diagrams for the optimized molecular geometries of **L1Et**, **L8*t*BuPt** and **L10BisIm** while Fig. 4 contains those for **L2Ph**, **L6Me** and **L7*t*BuPh**, respectively. The HOMO frontier orbitals were mainly found to be concentrated on the imidazole rings (Figs. 3 and 4) and this may explain why the phenol substituent perturbations produced greater effects on pK_as of imidazole base than on the phenolic hydroxyl function. Two alternative forms of orbitals alignments were observed to exist in the HOMO and HOMO-1 levels and which are energetically close (0.045–0.945 eV). The electron densities were either aligned across the N–N–O hetero atom axis (e.g. Fig. 3(b) and (e); Fig. 4 (b), (e), (h)) or along the length of the molecule (Fig. 3(h)). It is noteworthy that the former case occurred in the HOMO level of all studied molecules except for the symmetrical **L10BisIm** where the later case formed the HOMO level. This observation supports the importance of intramolecular hydrogen bonding in this family of molecules unlike for **L10BisIm** where such bonding was not applicable. This view was also supported by the lower dipole moments or lowest difference between N-atom charge densities for compounds **L9Anthr** and **L10BisIm** (Fig. 2, Table 2). The imidazole ring substituents in this work contributed to shift the imidazole aromatic π-density towards the 4,5-carbons in the order phenanthroleneyl > 4,5-diphenyl > 4,5-diethyl. This order is opposite to the effect of 4,5-substituent on donor strength of imidazole nitrogen base. Therefore, it is suggested that, from the ionization constant of imidazole-containing biomacromolecules, nature of unknown

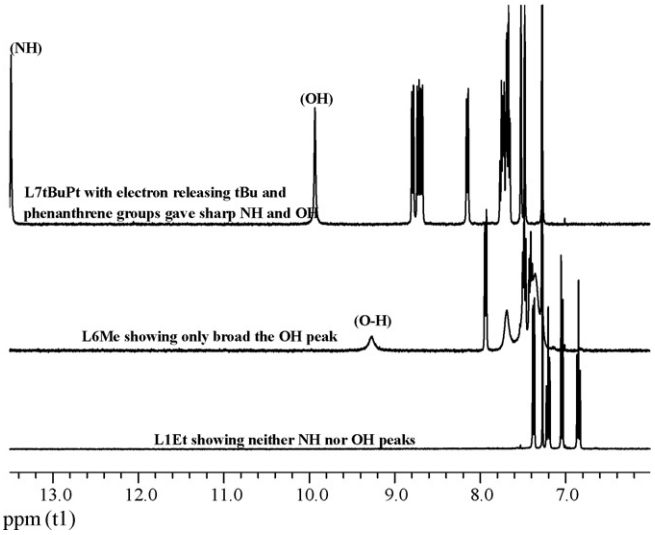

Fig. 6. ^{1}H NMR spectra for compounds **L1Et**, **L6Me** and **L8*t*BuPt** in deuterated chloroform.

substituents and donor property of such imidazole base can be predictable.

3.3. FTIR and ^{1}H NMR spectral characteristics of active protons

The observed FTIR and ^{1}H NMR data are presented in Table 1. The imidazole (N–H) and the phenolic (O–H) protons, which are the two types of active protons present in the investigated molecules, were spectroscopically compared for potentially useful information derivable from FTIR and ^{1}H NMR data and that can aid understanding of substituent effects on protonation–deprotonation equilibrium characteristics as well as intramolecular H-bonding properties. Solid-state FTIR signals for the phenolic protons ν_{O-H} were generally weaker and very broad unlike the sharp peaks found for the imidazole N–H peaks in all cases. Confirmation of this conclusion was obtained from spectral overlay for **L8*t*BuPt** and its oxazole analogue, which was obtained as a second product in the synthesis of **L8*t*BuPt** (Fig. 4(a)) [36]. In fact, the O–H signals for compound with relatively stronger imidazole donor strengths (e.g. **L2Ph**, **L3*m*-OMe**, **L4*p*-OMe** and **L5Naph**; Fig. 4(b) and (c)) were not observed, which is in agreement with weakening of O–H vibrations as a result of stronger intramolecular hydrogen bonding in such cases. The ^{1}H NMR properties of the molecules also provided support for observed trends. It is notable that, under similar conditions, **L8*t*BuPt** gave very sharp signals for the imidazole N–H and phenolic O–H protons (Fig. 5). This suggests weak or absence of intramolecular H-bonding and low donor strength of the imidazole base. Therefore, it could be concluded that electron-releasing substituents on the phenol ring and/or electron-withdrawing substituents on 4,5-imidazole carbons negatively affects donor strengths/coordination chemistries of 2-(1H-imidazol-2-yl)phenols, and vice versa (Fig. 6).

4. Conclusion

New imidazole based molecules were synthesized, characterized and used to investigate the effects of parameters such as different substituents and intramolecular interactions on ionization constant values. The pK_a values observed for the imidazole nitrogen base ranged from 1.11 to 6.64 contrary to the general believe that pK_a values for imidazole nitrogen base is usually around pK_a = 6. The phenol hydroxyl functions in the studied molecules showed lesser sensitivity to substituents effects unlike the imidazole base. While electron-releasing substituents produced increase in protonation–deprotonation pK_as for the hydroxyl group, values for the imidazole base were mainly affected by polarization of the imidazole ring aromaticity across the 2-imidazole carbon to 4,5-imidazole carbons axis of the imidazole ring. Therefore, it was concluded that electron-releasing substituents on the phenol ring and/or electron-withdrawing substituents on 4,5-imidazole carbons negatively affects donor strengths/coordination chemistries of 2-(1H-imidazol-2-yl)phenols, and vice versa. Experimental findings in this work also show that the substituents on the phenol ring significantly affect the donor strength of the imidazole base. The understanding of pK_a variation on account of electronic effects of different substituents in this work should aid the understanding of biochemical properties of imidazole-dependent biomolecules. The nature of substituent functionalities in the environments of imidazole donors present in biomacromolecules such as metalloenzymes, nucleotides, etc., can also be predicted based on ionization constant determinations.

Acknowledgements

The authors thank the Chinese Academy of Sciences and the Academy of Sciences for the Developing World (Italy) for granting postgraduate fellowship (CAS-TWAS) to AOE. The authors are also grateful to Redeemer's University – Nigeria for granting study leave to AOE.

References

[1] T.W. Birch, L.J. Harris, Biochem. J. 24 (1930) 564.
[2] J.P. Greenstein, J. Biol. Chem. 93 (1931) 479.
[3] G.M. Richardson, Biochem. J. 27 (1933) 1036.
[4] P.V. Oliferenko, A.A. Oliferenko, G. Poda, V.A. Palyulin, N.S. Zefirov, A.R. Katritzky, J. Chem. Inf. Model. 49 (1999) 634.
[5] W.N. Lipscomb, N. Strter, Chem. Rev. 96 (1996) 2375.
[6] T.J. Meyer, M.H.V. Huynh, H.H. Thorp, Angew. Chem. Int. Ed. 46 (2007) 5284.
[7] M. Voicescu, Y. El Khoury, D. Martel, M. Heinrich, P. Hellwig, J. Phys. Chem. B 113 (2009) 13429.
[8] J.C. Freys, G. Bernardinelli, O.S. Wenger, Chem. Commun. 2008 (2008) 4267.
[9] T. Irebo, S.Y. Reece, M. Sjodin, D.G. Nocera, L. Hammarström, J. Am. Chem. Soc. 129 (2007) 15462.
[10] G.T. Castro1, S.E. Blanco, O.S. Giordano, Molecules 5 (2000) 426.
[11] T. Gladysheva, J. Liu, B.P. Rosen, J. Biol. Chem. 271 (1996) 33256.
[12] C. Öğretir, H. Berber, O. Asutay, J. Chem. Eng. Data 46 (2001) 1540.
[13] N.C. Marziano, C. Tortatoa, R. Bertani, J. Chem. Soc. Perkin Trans. 2 (1992) 955.
[14] J.L. Décout, M.C. Maurel, Orig. Life Evol. Biosph. 23 (1993) 299.
[15] G. Ataie, A.A. Moosavi-Movahedi, A.A. Saboury, G.H. Hakimelahi, J.R. Hwu, S.C. Tsay, Int. J. Biol. Macromol. 27 (2000) 29.
[16] S. Yan, Y. Bu, J. Phys. Chem. 108 (2004) 13874.
[17] M.S.A. Hamza, X. Zou, R. Banka, K.L. Brown, R.v. Eldik, Dalton Trans. 2005 (2005) 782.
[18] H.-O. Bertrand, M.-O. Christen, J.-L. Burgot, Analyst 120 (1995) 2639.
[19] L. Benisvy, A.J. Blake, D. Collison, E.S. Davies, C.D. Garner, E.J.L. McInnes, J. McMaster, G. Whittaker, C. Wilson, Chem. Commun. 2001 (2001) 1824.
[20] C. Foulon, C. Danel, C. Vaccher, S. Yous, J.-P. Bonte, J.-F. Goossens, J. Chromatogr. A 1035 (2004) 131.
[21] Y.-X. Yan, Y.-H. Sun, L. Tian, H.-H. Fan, H.-Z. Wang, C.-K. Wang, Y.-P. Tian, X.-T. Tao, M.-H. Jiang, Opt. Mater. 30 (2007) 423.
[22] K. Feng, F.-L. Hsu, D.V. DerVeer, K. Bota, X.R. Bu, J. Photochem. Photobiol. 165 (2004) 223.
[23] M.-J. Han, Y.-M. Chen, K.-Z. Wang, N. J. Chem. 32 (2008) 970.
[24] F. Gao, X. Chen, F. Zhou, L.-P. Weng, L.-T. Guo, M. Chen, H. Chao, L.-N. Ji, Inorg. Chim. Acta 362 (2009) 4960.
[25] L. Bu, T. Sawada, Y. Kuwahara, H. Shosenji, K. Yoshida, Dyes Pigments 59 (2003) 43.
[26] J.A. Mondal, G. Ramakrishna, A.K. Singh, H.N. Ghosh, M. Mariappan, B.G. Maiya, T. Mukherjee, D.K. Palit, J. Phys. Chem. 108 (2004) 7843.
[27] R.-Y. Wang, W.-L. Jia, H. Aziz, G. Vamvonuis, S. Wang, N.-X. Hu, Adv. Funct. Mater. 15 (2005) 1483.
[28] W. Lin, L. Long, L. Yuan, Z. Cao, B. Chen, W. Tan, Org. Lett. 10 (2008) 5577.

[29] K.-Z. Wang, L.-H. Gao, G.-Y. Bai, L.-P. Jin, Inorg. Chem. Commun. 5 (2002) 841.
[30] A.O. Eseola, M. Zhang, J.-F. Xiang, W. Zuo, Y. Li, J.A.O. Woods, W.-H. Sun, Inorg. Chim. Acta, doi:10.1016/j.ica.2009.1002.1026, in press.
[31] Y.-P. Tong, S.-L. Zheng, X.-M. Chen, Eur. J. Inorg. Chem. 44 (2005) 3734.
[32] R.M. Tarkka, X. Zhang, S.A. Jenekhe, J. Am. Chem. Soc. 118 (1996) 9438.
[33] F. Liang, L. Wang, D. Ma, X. Jing, F. Wang, Appl. Phys. Lett. 81 (2002) 4.
[34] I.J. Rhile, T.F. Markle, H. Nagao, A.G. DiPasquale, O.P. Lam, M.A. Lockwood, K. Rotter, J.M. Mayer, J. Am. Chem. Soc. 128 (2006) 6075.
[35] T.F. Markle, I.J. Rhile, A.G. DiPasquale, J.M. Mayer, Proc. Natl. Acad. Sci. 105 (2008) 8185.
[36] A.O. Eseola, W. Li, R. Gao, M. Zhang, X. Hao, T. Liang, N.O. Obi-Egbedi, W.-H. Sun, Inorg. Chem. 48 (2009) 9133, and supporting information there in.
[37] K. Das, N. Sarkar, A.K. Ghosh, D. Majumdar, D.N. Nath, K. Bhattacharyya, J. Phys. Chem. 98 (1994) 9126.
[38] M.A. Ríos, M.C. Ríos, J. Phys. Chem. A 102 (1998) 1560.
[39] S. Yan, Y. Bu, Z. Cao, P. Li, J. Phys. Chem. A 108 (2004) 7038.
[40] J.S. Coleman, L.P. Varga, S.H. Mastin, Inorg. Chem. 9 (1970) 1015.
[41] M.J. Frisch, G.W. Trucks, H.B. Schlegel, G.E. Scuseria, M.A. Robb, J.R. Cheeseman, V.G. Zakrzewski, J.A. Montgomery Jr., R.E. Stratmann, J.C. Burant, S. Drapprich, J.M. Millam, A.D. Daniels, K.N. Kudin, M.C. Strain, O. Farkis, J. Tomasi, V. Barone, M. Cossi, R. Cammi, B. Mennucci, C. Pomelli, C. Adamo, S. Clifford, J. Ochterski, G.A. Petersson, P.Y. Ayala, Q. Cui, K. Morokuma, D.K. Malick, A.D. Rabuck, K. Raghavachari, J.B. Foresman, J. Cioslowski, J.V. Ortiz, B.B. Stefanov, G. Lui, A. Laishenko, P. Piskorz, I. Komoromi, R. Gomperts, R.L. Martin, D.J. Fox, T. Keith, M.A. Al-Laham, C.Y. Peng, A. Nanayakkara, C. Gonzalez, M. Challacombe, P.M.W. Gill, B. Johnson, W. Chen, M.W. Wong, J.L. Andres, C. Gonzalez, M. Head-Gordon, E.S. Repogle, J.A. Pople, GAUSSIAN 98, Revision A.6, Gaussian Inc., Pittsburgh, PA, 1998.